PROGRESS IN PHOTOVOLTAICS: RESEARCH AND APPLICATIONS
Prog. Photovolt: Res. Appl. 2008; **16**:503–508
Published online 1 May 2008 in Wiley InterScience (www.interscience.wiley.com) DOI: 10.1002/pip.834

Research

Concentrator Multijunction Solar Cell Characteristics Under Variable Intensity and Temperature

Geoffrey S. Kinsey*,†, Peter Hebert, Kent E. Barbour, Dmitri D. Krut, Hector L. Cotal and Raed A. Sherif
Spectrolab, Inc., Sylmar, CA 91342, USA

The performance of multijunction solar cells has been measured over a range of temperatures and illumination intensities. Temperature coefficients have been extracted for three-junction cell designs that are in production and under development. A simple diode model is applied to the three-junction performance as a means to predict performance under operating conditions outside the test range. These data may be useful in guiding the future optimization of concentrator solar cells and systems. Copyright © 2008 John Wiley & Sons, Ltd.

KEY WORDS: photovoltaic cell measurements; solar energy

Received 27 December 2007; Revised 3 March 2008

INTRODUCTION

Concentrator photovoltaic (CPV) systems using multijunction solar cells promise to deliver electrical power at a lower cost than will be possible with traditional flat-plate systems. To realize this promise, the CPV system must be designed to extract maximum performance from the expensive multijunction solar cells while minimizing system costs associated with the concentrating optics, temperature control, and the remaining balance-of-system costs. In general, cell conversion efficiency will increase with concentration until series resistance begins to limit performance. Multijunction concentrator cells have recently achieved very high performance levels, with a record efficiency of 40·7% at 240 suns, exceeding 40% conversion efficiency.[1] Candidate CPV systems typically become more economically viable as the concentration design point is increased, to 300 suns and above,[2] so it is important to characterize and optimize cell performance in this concentration range. In order to translate the high multijunction cell performance into low system-level energy costs, a convergence of multijunction cell and CPV system design must be obtained. Field testing of several prototype CPV systems using multijunction cells is currently underway; the resulting data will be used to optimize both future multijunction cell and overall CPV system design. Indoor testing using calibrated solar simulators has been used to evaluate multijunction solar cell performance over a temperature range of 0–120°C and an illumination intensity range from less than 1× intensity up to 1000×. Throughout this paper, 1× is defined as 0·09 W/cm^2, ASTM G173-03 standard spectrum. Temperature coefficients at multiple concentration levels have been extracted and compared to theoretical predictions. The multijunction solar cell devices under test were the ‘‘concentrator, 1st-generation multi-

* Correspondence to: Geoffrey S. Kinsey, Spectrolab, Inc., Sylmar, CA 91342, USA.
†E-mail: gkinsey@spectrolab.com

junction'' (C1MJ) and prototype ''concentrator, 2nd-generation multijunction'' (C2MJ) cells. The C1MJ cell has been in production since 2006; C1MJ cells have passed a qualification program and are now installed in several CPV systems around the world. Several design variations are being evaluated for the C2MJ cell due to be in production in 2008. The particular prototype C2MJ cell evaluated in this work has a top subcell with a wider band gap, resulting in a higher voltage output than the C1MJ. This comes at the price of reduced current output under atmospheric conditions of high effective air mass (where the top subcell will be unable to absorb sufficient light to match the current output of the other two subcells). The characteristics of these cells under controlled test conditions inform the determination of optimal operating conditions for present and future CPV system designs.[3,4]

The multijunction solar cell currently consists of three subcells grown monolithically via metal–organic vapor-phase epitaxy and connected in series using tunnel junctions (Figure 1). To determine how the multijunction cell will perform in operation, it is possible to treat this three-junction series-connected cell as a single diode. This approach is often used by CPV system designers to predict multijunction performance under various temperature and intensity conditions. Though the three subcell diodes in series, with two tunnel junctions, have a complicated structure than might be expected to deviate in performance from a single-diode model, in practice, the effects of this complex structure are most pronounced near the maximum power point. At the open-circuit voltage of the multijunction, where the net current flow is zero, empirical parameters such as temperature coefficients and effective ideality factor for a lumped diode may be extracted from variable intensity and temperature measurements. These parameters, in turn, may be used to extrapolate performance of the multijunction cell at higher concentrations and temperatures. The results that follow give some indication of both the potential and the limitations of this approach.

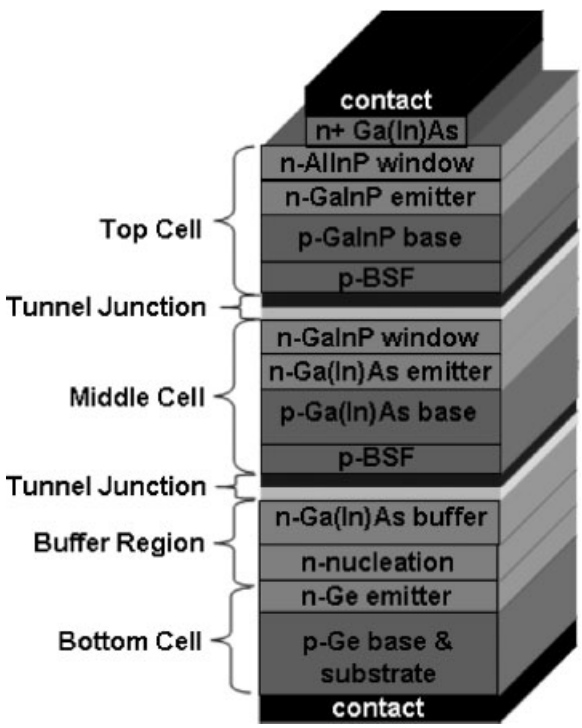

Figure 1. Lattice-matched multijunction solar cell

Variable intensity and temperature measurements were taken on C1MJ and one version of prototype C2MJ cells using indoor flash testing. A High-Intensity Pulsed Solar Simulator (HIPSS) was used as the illumination source. Via neutral density filters, the HIPSS is capable of spanning a concentration range below 100× up to 1000×. Characteristics at concentrations above 300× are the principle focus in the discussion below. The HIPSS simulators employ filtering of xenon sources to match the ASTM G173-03 terrestrial spectrum. This is the current baseline spectrum for production testing of CPV cells. The simulator output is calibrated using reference ''isotype'' single-junction cells traceable to standards measured by the National Renewable Energy Laboratory (NREL). The isotype single-junction cells have the same material composition as a full, three-junction multijunction, but are doped so that only either the top subcell or middle subcell is the active junction. Cell temperature was monitored using a thermocouple mounted adjacent to the solar cell on a heating/cooling block. During the flash test, the cell temperature is assumed to remain constant. Over the course of several months, three iterations of variable intensity and temperature testing (Tests ''A,'' ''B,'' and ''C'') were conducted in this study. The cell configuration is the CDO-100, which is a concentrator cell with dual ohmic contacts for cell assembly and a square aperture area of 100 mm^2. The CDO-100 is presently a common size for CPV systems, although considerations such as resistive power loss and optics costs make other sizes attractive as well. The metal grid pattern was optimized for operation under an intensity of 50 W/cm^2. Each test point is the mean of the performance of a small quantity of cells of each type (two in Test A, four in Test B, and six in Test C).

DOI: 10.1002/pip

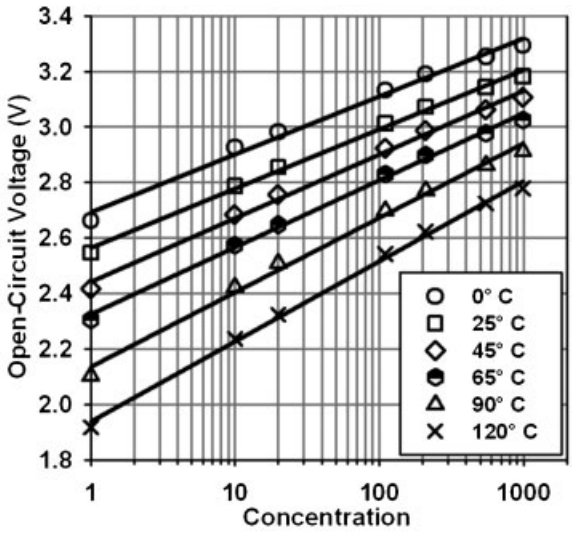

Figure 2. Open-circuit voltage as a function of intensity and temperature for a set of C1MJ cells during Test A. "1×" concentration is defined as 0·09 W/cm^2

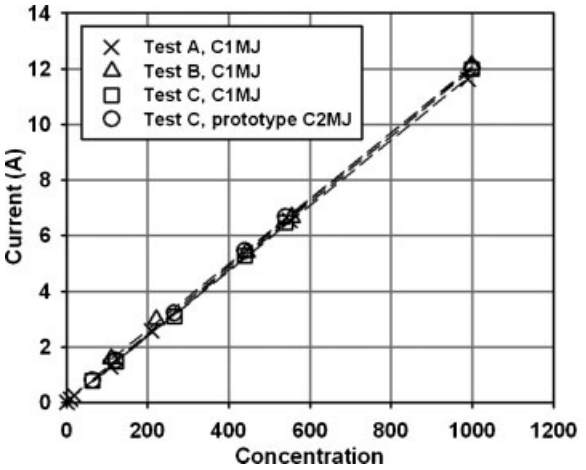

Figure 3. Short-circuit current at 25°C. The three-junction cells are linear with respect to single-junction calibration standards

C1MJ cells were measured in Test A and Test B; C1MJ & the prototype configuration of C2MJ were included in Test C.

RESULTS AND ANALYSIS

Open-circuit voltage operating characteristics are shown in Figure 2. The logarithmic fits to these data can be used to extract an effective mean ideality factor for the three subcells that compose the lumped diode. For a solar cell under illumination, the simple diode equation can be expressed as

$$J = J_0\left(e^{\frac{qV}{nkT}} - 1\right) - J_{\text{ph}} \tag{1}$$

where J is the current density, V the voltage, J_{ph} the photogenerated current density, J_0 the diode saturation current density, n the diode ideality factor, k the Boltzmann's constant, and T is the temperature. The photogenerated current density, J_{ph}, is nearly equal to the short-circuit current density, J_{sc}, of the solar cell, to a good approximation. The intensity was calibrated with the reference isotype cells that are assumed to have linear current dependence on intensity. As can be seen from Figure 3, the short-circuit current of the triple-junction cells is linear with respect to the single-junction calibration standards. It is therefore convenient to assume that the concentration at a given intensity (I) can be expressed as the ratio of the short-circuit current density to that at 1× intensity ($I_{X=1}$):

$$X = \frac{J_{\text{sc}}(I)}{J_{\text{sc}}(I_{X=1})} \tag{2}$$

Substituting J_{sc} for J_{ph} in Equation (1) and combining Equations (1) and (2) gives

$$V_{\text{oc}} = \frac{nkT}{q\log(e)} \cdot \log(X) + V_{\text{oc},X=1} \text{ for } e^{\frac{qV_{\text{oc},X=1}}{nkT}} >> 1, \frac{1}{X} \tag{3}$$

The first term in Equation (3) provides a means for extracting an ideality factor (n) at each temperature from the slope of logarithmic curve fits such as those in Figure 2. The ideality factors for three-junction cells are shown in Figure 4.

Variability in the ideality factor is attributable to multiple factors, including distributed diode effects,[5] differences in the junction profiles and current matching among the individual cells measured and, to a lesser extent, the measurement setup. Due to distributed diode effects and the probability of recombination within the subcell base regions, the ideality factor for the three junctions is typically greater than 3. In general, the ideality factor is expected to decrease as temperature (and intrinsic doping levels) increase,[6] but such a trend is not

DOI: 10.1002/pip

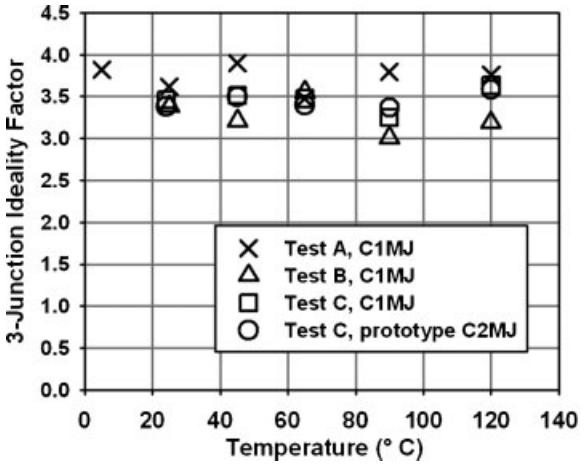

Figure 4. Average, effective ideality factor of three-junction cells, extracted from V_{oc} data

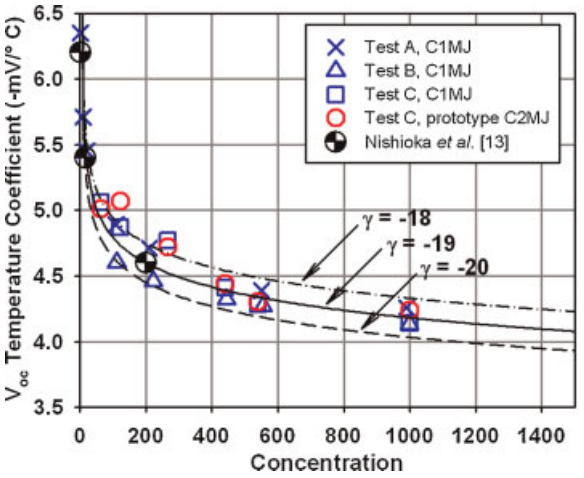

Figure 6. Open-circuit voltage temperature coefficients for multijunction cells. (The voltage decreases with increasing temperature.) Theoretical values using the simple diode assumption for several values of γ are shown

noticeable over this temperature range. As each subcell differs in structure and composition, the subcell ideality factor can be expected to vary. The ideality factors extracted here represents a mean value and therefore has limited relation to any one subcell. Nevertheless, the values extracted for the lumped diode model serve as bracketing conditions for modeling of multijunction cells.

Plotting the open-circuit voltage (V_{oc}) as a function of temperature (Figure 5) allows for the extraction of the open-circuit voltage temperature coefficients at various concentrations. Open-circuit voltage temperature coefficients of both cell configurations, for temperatures in the 0–120°C range, are shown in Figure 6.

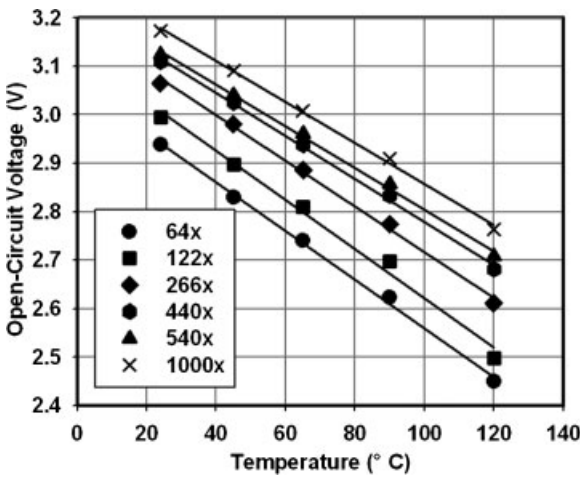

Figure 5. Open-circuit voltage as a function of intensity and temperature for a set of prototype C2MJ cells during Test C

Returning to Equation (1) and solving for the open-circuit voltage (V_{oc}) condition gives

$$V_{oc} = \frac{nkT}{q} \cdot \ln\left(\frac{J_{sc}}{J_0} + 1\right) \tag{4}$$

The temperature dependence of the reverse saturation current density (J_0) in each subcell can be determined assuming[7]

$$J_0 \propto T^{\left(3+\frac{\gamma}{2}\right)} e^{-\frac{E_g}{kT}} \tag{5}$$

where E_g is the appropriate subcell band gap and γ is used to represent the power-law temperature dependence of the ratio of diffusion coefficients to the minority carrier lifetimes. The temperature dependence of each subcell band gap,[8] and its resulting derivative, can be expressed as

$$E_g(T) = E_g(0) - \frac{\alpha T^2}{T + \beta} \tag{6}$$

$$\frac{\partial E_g}{\partial T} = -\frac{2\alpha T}{T + \beta} + \frac{\alpha T^2}{(T + \beta)^2} \tag{7}$$

Empirical values for α and β are available for the GaInP, GaInAs, and Ge materials in the three subcells.[9–11] As demonstrated in Reference[12], substitution of Equation (5) into Equation (4) and

DOI: 10.1002/pip

differentiation with respect to temperature results in

$$\frac{\partial V_{oc}}{\partial T} = -\frac{1}{T}\left(\frac{n}{q}\cdot E_g - V_{oc} + \frac{nkT}{q}\cdot\left(3+\frac{\gamma}{2}\right)\right) + \frac{nkT}{q}\cdot\frac{1}{J_{sc}}\cdot\frac{\partial J_{sc}}{\partial T} + \frac{n}{q}\cdot\frac{\partial E_g}{\partial T} \quad (8)$$

Empirical values are available for each of the terms in Equation (8) except for the γ term. The temperature dependence of the γ term depends on that of the underlying diffusion coefficients and carrier lifetimes. The expression for these terms is fairly complex[12] and the values are not well understood for the various materials involved. Accordingly, the γ term is often neglected in expressions for the reverse saturation current.[11,13] In this work, the γ term has been treated as a fitting factor; several values of γ inserted into Equation (8) yield the curves shown in Figure 6. The range of curves provides some prediction of cell performance above 1000×, where many future CPV systems are expected to operate.

Overall, the voltage temperature coefficients exhibit the expected decrease with concentration. This bodes well for future, high-concentration systems and implies a performance advantage with respect to silicon single-junction cells in these operating ranges.[14,15] As an example, at 65°C and 250×, a multijunction V_{oc} temperature coefficient of −4·6 mV/°C implies a 1·5% decrease in voltage with respect to that at 25°C; for a crystalline silicon cell under similar conditions, a 1·7% decrease is expected.[15] Given the larger voltage of the multijunction, this differential will widen at the higher concentrations at which multijunctions might be expected to displace silicon cells.

Representative curves for cell fill factor and efficiency as a function of concentration are shown in Figure 7. Up to approximately 200× concentration, the fill factor increases, proportional to the increase in open-circuit voltage. At higher concentrations, series resistance limits fill factor. In contrast, the efficiency peaks at 500×, as designed. This is due to the fact that the metal contact grid coverage fraction and resistive power loss can be optimized for a given target concentration. However, as a result of the fill factor limitation, the highest overall efficiencies are typically obtained below 300×, even with such grid optimization. Since CPV systems using multijunction cells become economical only at higher concentration, a principal focus of ongoing cell development is to minimize the various contributors of internal and external series resistance that contribute to fill factor limitations. It is desirable to shift the peak in fill factor toward 500×, where most current CPV systems are designed to operate. This will translate to a higher efficiency than is currently obtained for cells optimized for that concentration.

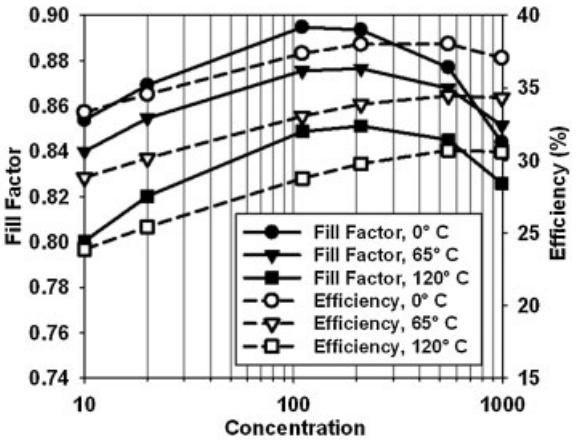

Figure 7. Fill factor compared to efficiency of C1MJ cells from Test A

Efficiency temperature coefficients are listed in Table I. The efficiency temperature coefficient results are not as consistent as those for open-circuit voltage.

Table I. Efficiency temperature coefficients (absoulte %/°C)

X	Test A	Test B	Test C	
	C1MJ	C1MJ	C1MJ	Prototype C2MJ
10	−0·081			
20–70	−0·078		−0·083	−0·085
110–120	−0·072	−0·074	−0·062	−0·070
210–270	−0·069	−0·039	−0·069	−0·071
440		−0·041	−0·051	−0·056
540–560	−0·062	−0·044	−0·046	−0·046
990–1000	−0·055	−0·051	−0·035	−0·047

DOI: 10.1002/pip

This is due to a host of factors, including the compound contributions of the open-circuit voltage and fill factor, changes in the current ratio between subcells with temperature, and variable parasitic series resistance effects in the measurement setup. Nevertheless, the expected trend toward lower temperature coefficients at higher concentrations is observed.

CONCLUSION

Multijunction solar cells have been characterized across a range of temperatures and illumination intensities. Application of a lumped diode model to the three-diode structure provides insight into expected performance. The cell characteristics may be used to inform cell development and CPV system design. Performance results are encouraging for near-term improvement of multijunction operation in high-concentration CPV field systems.

REFERENCES

1. King RR, Law DC, Edmondson KM, Fetzer CM, Kinsey GS, Yoon H, Sherif RA, Karam NH. 40%-efficient metamorphic GaInP/GaInAs/Ge multijunction solar cells. *Applied Physics Letters* 2007; **90**: 183516.
2. Verlinden PJ, Lewandoswki A, Bingham C, Kinsey GS, Sherif RA, Lasich JB. Performance and reliability of mulit-junction III-V dense array modules for concentrator dish and central receiver applications. *Proceedings of the IEEE 4th World Conference on Photovoltaic Energy Conversion*, 2006; **1**: 592–597.
3. Cotal HL, Sherif RA. Temperature dependence of the IV parameters from triple junction GaInP/InGaAs/Ge concentrator solar cells. *Proceedings of the IEEE 4th World Conference on Photovoltaic Energy Conversion*, 2006; **1**: 845–848.
4. Nishioka K, Takamoto T, Agui T, Kaneiwa M, Uraoka Y, Fuyuki T. Evaluation of temperature characteristics of high-efficiency InGaP/InGaAs/Ge triple-junction solar cells under concentration. *Solar Energy Materials and Solar Cells* 2005; **85**: 429–436.
5. Araki K, Yamaguchi M, Imaizumi M, Matsuda S, Takamoto T, Kurita H. AM0 concentration operation of III-V compounds solar cells. *28th IEEE Photovoltaic Specialists Conference*, 2000; 968–971.
6. Verschraegen J, Burgelman M, Penndorf J. Temperature dependence of the diode ideality factor in $CuInS_2$-on-Cu-tape solar cells. *Thin Solid Films* 2005; **480–481**: 307–311.
7. Bhattacharya P. *Semiconductor Optoelectronic Devices*. Prentice-Hall: Englewood Cliffs, NJ, 1994; 178.
8. Varshni YP. Temperature dependence of the energy gap in semiconductors. *Physica* 1967; **34**(1): 149–154.
9. Swaminathan V, Macrander AT. *Materials Aspects of GaAs and InP Based Structures*. Prentice-Hall: Englewood Cliffs, NJ, 1991; 18.
10. Van Zeghbroeck BJ. *Principles of Semiconductor Devices*. 1997. Available at http://ece-www.colorado.edu/∼bart/book/eband5.htm
11. Fan JCC. Theoretical temperature dependence of solar cell parameters. *Solar Cells* 1986; **17**: 309–315.
12. Nishioka K, Takamoto T, Agui T, Kaneiwa M, Uraoka Y, Fuyuki T. Annual output estimation of concentrator photovoltaic systems using high-efficiency InGaP/InGaAs/Ge triple-junction solar cells based on experimental solar cell's characteristics and field-test meteorological data. *Solar Energy Materials and Solar Cells* 2006; **90**(1): 57–67.
13. Friedman DJ. Modeling of tandem cell temperature coefficients. *25th IEEE Photovoltaic Specialists Conference*, 1996; 89–92.
14. Zhao J, Wang A, Robinson SJ, Green MA. Reduced temperature coefficients for recent high-performance silicon solar cells. *Progress in Photovoltaics: Research and Applications* 1994; **2**(3): 221–225.
15. Yoon S, Garboushian V, Roubideaux D. Reduced temperature dependence of high-concentration photovoltaic solar cell open-circuit voltage (Voc) at high concentration levels. *24th IEEE Photovoltaic Specialists Conference*, 1994; **2**: 1500–1504.

DOI: 10.1002/pip